JOC Article

Control of Stereoselective Protonation of Enols[1,2]

Howard E. Zimmerman* and Jie Cheng

Chemistry Department, University of Wisconsin, Madison, Wisconsin 53706

zimmerman@chem.wisc.edu

Received August 1, 2005

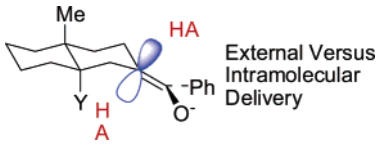

A decalyl framework with a siloxy enolic moiety and proximate proton transferring groups was synthesized. On enolate generation with fluoride two competitive reaction modes were possible: (a) intermolecular protonation, and (b) intramolecular proton transfer by the proximate group. Control of the protonation stereochemistry proved possible by varying the proximate group and by changing the acidity of the medium. With the groups $-CH_2OH$, $-CH{=}O$, and $-CH_2OCH_2OCH_3$ as the proximate groups, only intermolecular proton transfer was observed with no dependence on acidity. In contrast, with $-COO^-$ and COOH, only intramolecular protonation resulted but again with no dependence on acidity of the medium. In contrast, with $-CH_2NH_2$ as the proximate group, intramolecular proton transfer predominated with a dependence on the effective pH of the medium. A kinetic analysis provided a linear-log relationship of the ratio of the two stereoisomers with the medium acidity. The analysis revealed that two acetic acid molecules are involved in providing the proton to the enolate moiety. A theoretical analysis was developed paralleling the experimental results. In the ketonization transition state, the hybridization was shown to be close to sp^2 hybridized at the α-enolate carbon.

Introduction

Beginning in 1956, one research objective has been to understand the stereochemistry of protonation of mesomeric anions such as enolates and nitronates.[3] In our original paper and in the many publications[4] following, we noted that the process is highly exothermic with a nearly planar enolic system in the transition state. Protonation occurs from the less hindered face of the delocalized enolate. The consequence is that for the myriad of reactions proceeding via enolic intermediates the less stable diastereomeric product is formed under kinetically controlled conditions. Some examples are conjugate additions to enones, decarboxylation of β-ketoacids and malonic acids, dehalogenation of α-haloketones, deprotonation-protonation of ketones and esters, Birch−Barton−Stork lithium-ammonia reduction of enones, and nucleophilic addition to ketenes. Thus, in each case less hindered protonation controls the reaction stereochemistry.

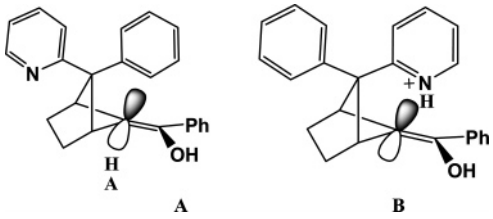

FIGURE 1. Two Diastereomeric Transition States with **A** giving preferred intermolecular protonation and **B** giving preferred intramolecular protonation.

Very recently we have reported a reversal of the phenomenon with protonation of the more hindered side of the enolic system by use of a proximate 2-pyridyl moiety capable of proton delivery.[5,6] One example is depicted in Figure 1 where diastereomer **A** undergoes protonation to afford the less stable diastereomeric benzoyl ketone while diastereomer **B** is protonated intramolecularly to afford the more stable benzoyl isomer.

The intent of the present study was to determine if the phenomenon was more general and whether groups other than 2-pyridyl could serve to protonate intramolecularly. For this purpose we selected the decalyl system with an exocyclic enolic

(1) This is our publication 279.
(2) For publication 278 and a preliminary report of some of our early results, see: Zimmerman, H. E.; Cheng, J. *Org. Lett.* **2005**, *7*, 2595−2597.
(3) Zimmerman, H. E. *J. Org. Chem.* **1955**, *20*, 549−557.
(4) (a) See ref 4b for early references. (b) Zimmerman, H. E. *Acc. Chem. Res*. **1987**, *20*, 263−268. (c) Zimmerman, H. E.; Wang, P. J. *J. Org. Chem.* **2003**, *68*, 9226−9232.

10.1021/jo051611i CCC: $33.50
Published on Web 01/07/2006

SCHEME 1. Synthesis of Required Compounds Where Y Is Carboxyl

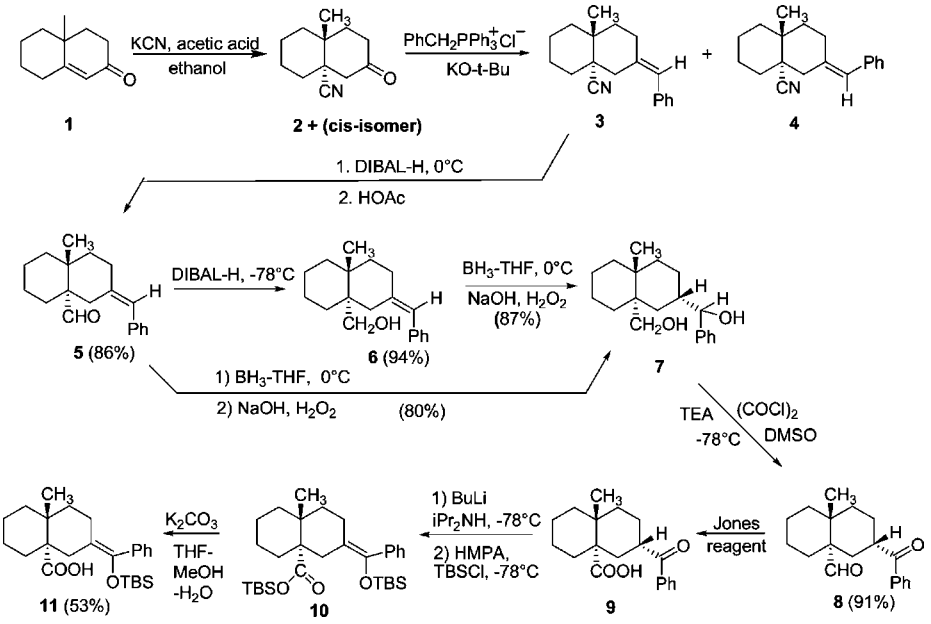

SCHEME 2. Synthesis of the MOMOM Derivative

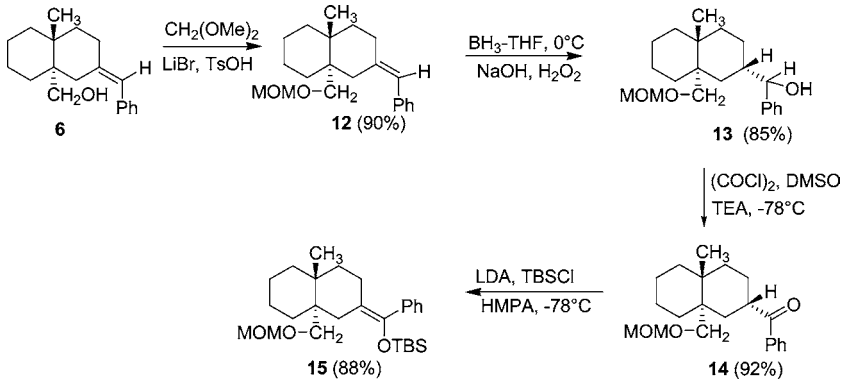

system at carbon 2 and potential proton delivery groups Y at carbon 9; note the general structure **C**.

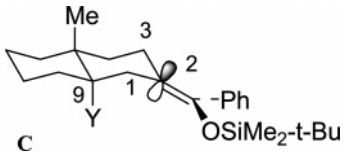

C

Results

Synthesis of Reactants. Scheme 1 outlines the synthesis of the first silyl enol ether required, namely, where the group Y is carboxyl. The synthesis had several steps of particular interest. In the case of cyanide addition to the known[7a] octalone **1**, both[7b] stereoisomeric cyanoketones **2** were obtained. However, only the trans stereoisomer was employed for the subsequent Wittig reaction. Again, two stereoisomeric products, **3** and **4**, resulted (NOE stereochemical assignment). Both proved of use subsequently. In the conversion of aldehyde **5** to diol **7**, the two-step procedure could be circumvented by the one-step hydroboration-oxidation converting **5** directly to **7**. The desired axial hydroxybenzyl group resulted nicely from the less hindered exo-hydroboration stereochemistry. Interestingly, oxidation of hydroxybenzyl diol **7** to benzoyl ketone **8** proved unsuccessful with the usual oxidants, Jones and Collins reagents, but proceeded nicely and without benzoyl epimerization under Swern condition. Collins conditions led to oxidation of the hydroxymethylene group to carboxyl and rapid lactonization with the benzylic hydroxyl. The Jones conditions afforded a dimeric ester. LDA silation of ketone **9** led to the unusually stable silyl ester **10**, which required selective basic desilation to afford the desired hydroxymethylene silyl enol ether **11**.

The synthesis of the methoxymethoxymethylene (MOMOM) derivative **15** is outlined in Scheme 2. Hydroboration of the styryl bond proved possible without disturbance of the MOMOM group. Again, the stereochemistry of hydroboration resulted from exo attack on the decalyl system to afford diastereomer **13** with its axial hydroxybenzylic substituent. Similarly, Swern oxidation nicely gave selective benzylic oxidation. Finally, for reasons to be considered subsequently,

(5) (a) Zimmerman, H. E.; Ignatchenko, A. *J. Am. Chem. Soc.* **1998**, *120*, 12992−12993. (b) Zimmerman, H. E.; Ignatchenko, *J. Org. Chem.* **1999**, *64*, 6635−6645.

(6) (a) Zimmerman, H. E.; Wang, P. *Org. Lett.* **2002**, *4*, 2593−2595. (b) Zimmerman, H. E.; Wang, P. *J. Org. Chem.* **2002**, *69*, 9216−9226.

(7) (a)Heathcock, C. H.; Ellis, J. E.; Mcmurry, J. E.; Coppolino, A. *Tetrahedron Lett.* **1971**, *52*, 4995−4996. (b) Banerjee, D. K.; Angadi, V. B. *Tetrahedron* **1965**, *21*, 281−289.

SCHEME 3. Synthesis of Aldehyde and Hydroxymethylene Enol Ethers

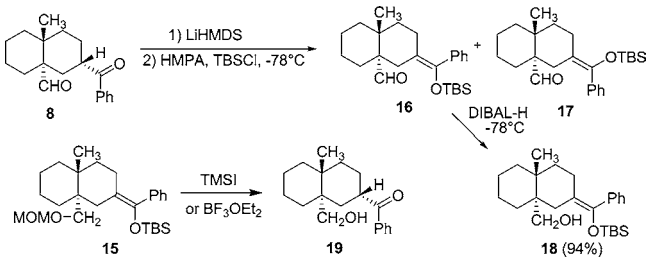

SCHEME 4. Synthesis of the Decalyl Aminomethylene Silyl Enol Ether

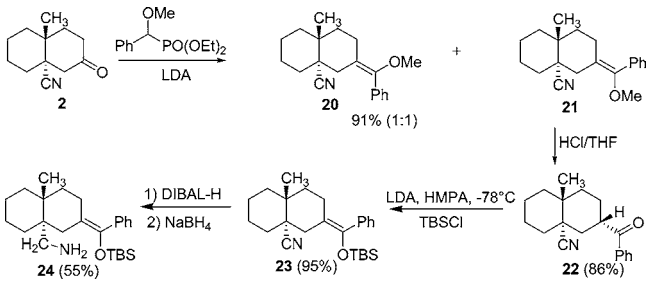

the axial benzoyl configuration of ketone **14** proved ideal for α-proton removal to afford the required silyl enol ether **15**.

At this point aldehyde **16** and hydroxymethylene **18** were prepared as outlined in Scheme 3. Keto aldehyde **8** proved to be a suitable starting point. In both cases the Z siloxy enol ether **16** was selected for subsequent study. In the conversion of benzoyl ketone **8** to the silyl enol ether stereoisomers **16** and **17**, initially LDA was employed as the base and afforded a 50% yield.

The problem with LDA as a base was its delivery of hydride to reduce the carboxyaldehyde moiety. However use of hexamethyldisilazide led to an improved yield of 82%, forming the cis and trans isomers in a 2:1 ratio. Since acid deprotection of the MOMOM group led to desilylation to afford **19**, the alternative DIBAL reduction of aldehyde **16** was employed, which nicely led to hydroxymethyl silyl enol ether **18**.

For the synthesis of the last desired silyl enol ether **24** (note Scheme 4), a Horner−Wadsworth−Emmons reaction of cyanoketone **2** with diethyl 1-methoxy-1-phenylmethylphosphonate furnished the methyl vinyl ethers **20** and **21**, which readily underwent acidic hydrolysis to give the cyano benzoyl product **22**. Deprotonation and silylation of the benzoyl compound **22** gave the cyano silyl enol ether **23**, which was reduced by DIBAL-H and $NaBH_4$ to provide the desired amino silyl enol ether **24**.

The configuration of the *Z*-isomer of **16** was determined by X-ray analysis. This identification was of interest since it led to suggesting the configurations of the remaining members of the series. Thus the dimethyl-*tert*-butylsilyl moiety had distinctive NMR differences between the *Z*- and *E*-stereoisomers as detailed in the Table 1. In brief, the NMR shift difference between the two methyl peaks seemed characteristically larger for the *Z*-isomer. This was not critical since (vide infra) the protonation was independent of *Z* versus *E* configuration.

Reactivity and Stereochemistry of the Enolic Species. On generation from the silyl enol ether precursor **18** the enolate in the hydroxymethylene case led almost exclusively to the axial benzoyl tautomer **19**. Over a range of 0.11−1.43 M acetic acid, the initial ratio of axial to equatorial isomers of 32:1 became 99:1. Thus, equatorial protonation corresponded to 97% throughout the change in acidity. Note Table 2, eq 1, and Figure 2. Parallel behavior was encountered when hydroxymethylene was replaced by the MOMOM group; again note Table 1, eq 1, and Figure 2. Where the transferring group was carboxyaldehyde, both cis and trans silyl ethers were available, but again these led overwhelmingly to the axial benzoyl diastereomer. Most significantly, both stereoisomeric silyl enol ethers afforded

TABLE 1. NMR Difference of Silyl Enol Ethers

compound	chemical shift of two methyl groups in the TBS group (ppm)		shift difference between two methyls (ppm)
11 (*Z*-carboxylic acid)	−0.18	−0.38	0.20
15 (*Z*-MOMOM)	−0.14	−0.30	0.16
16 (*Z*-carboxyaldehyde)	−0.15	−0.31	0.16
17 (*E*-carboxyaldehyde)	−0.17	−0.27	0.10
18 (*Z*-hydroxymethylene)	−0.05	−0.40	0.35
24 (*Z*-aminomethylene)	−0.1	−0.30	0.20

TABLE 2. Acid Dependence in Ketonization with Different Groups; Intramolecular versus Intermolecular Reactivity[a]

[HOAc] (M)	COOH	*Z*-CHO	*E*-CHO	CH_2OH	MOMOM[b]	CH_2NH_2[c]
0.05						47:53
0.11	97:3	6:94	6:94	3:97	4:96	70:30
0.21	98:2	5:95	6:94	2:98	4:96	83:17
0.37	98:2	5:95	5:95	2:98	2:98	86:14
0.73	99:1	3:97	4:96	1:99	1:99	93:7
1.43	99:1	1:99	2:98	1:99	1:99	

[a] All runs in THF. [b] MOMOM = CH_2OCH_2OMe. [c] Slope = 0.93 and intercept = 1.25 from the plot of $\log(P_{int}/P_{ext})$ vs log[AcOH] (note Figure 3).

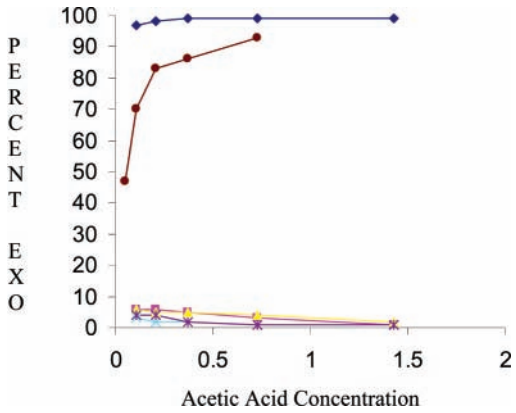

FIGURE 2. Percent of *exo* product versus acetic acid concentration: (blue ◆) COOH, (red ●) CH_2NH_2, (black ∗) MOMOM, (pink ■) *Z*-CHO, (light blue ■) $HOCH_2$, (yellow ▲) E-CHO.

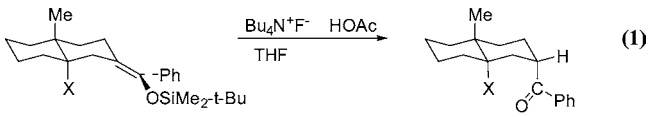

(1)

18 X = CH_2OH
16 X = CH=O (Z)
17 X = CH=O (E)
15 X= $MeOCH_2OCH_2$

19 X = CH_2OH
8 X = CHO
8 X = CHO
14 X = $MeOCH_2OCH_2$

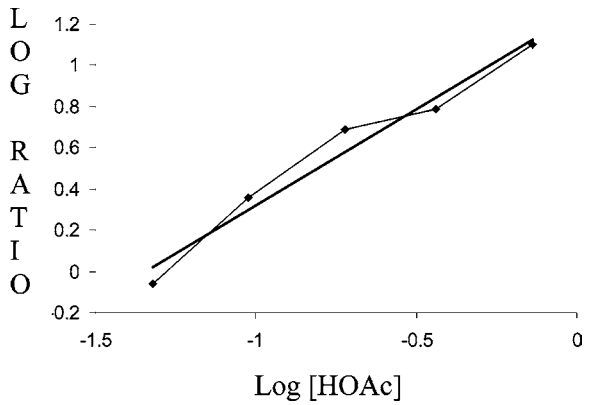

FIGURE 3. Plot of the log of the product ratio versus the log of the acid concentration.

TABLE 3. log(P_{int}/P_{ext}) versus log[AcOH] of the Aminomethylene Case

log[AcOH]	log(P_{int}/P_{ext})
−1.32	−0.06
−1.022	0.36
−0.721	0.688
−0.438	0.788
−0.136	1.1

the same stereoselectivity within experimental error (i.e., 1% deviation, Table 2 and eq 1). Hence, with hydroxymethylene, methoxymom, and carboxaldehyde groups, the preferred reaction stereochemistry derived from external protonation to afford the less stable axial benzoyl stereoisomer.

This is in accord with the normal course of kinetic protonation as originally described in 1956,[3] in our subsequent studies,[4] and in the multitude of subsequent literature examples.

In contrast, where the substituent was carboxyl or aminomethylene, intramolecular proton transfer was encountered. In the carboxyl case in DMSO, the enol derived from silyl enol ether **11** reacted with intramolecular proton transfer independent of acidity as controlled by a lithium acetate/acetic acid buffer with the LiOAc:HOAc ratio ranging from 0.5:1 to 8:1. Similarly, in THF with just acetic acid as the proton source, the stereochemistry was intramolecular to afford **25**. Note Table 2 and eq 2.

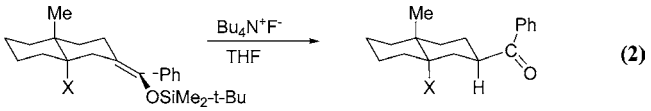

(2)

Remarkably, with aminomethylene as the transferring group (note eq 2), the reaction stereochemistry proved to be dependent on the medium acidity, although giving predominately intramolecular transfer throughout. The acid dependence is shown in Table 2, eq 2 and also in the logarithmic plot in Figure 3. Interestingly, when phenol was substituted for acetic acid as the proton source, the stereochemistry was reversed with intermolecular protonation predominating 5:1 as in eq 1.

Reaction Kinetics. In the aminomethylene case, as the acetic acid concentration was increased, the reaction gave more intramolecular protonation product. To understand this, we turned to a kinetic study. In our earlier studies[5,6] we noted that one can interpret log plots of the type given in Figure 3 (see also Table 3). Thus, if k_{int} is the rate constant for formation of benzoyl product by intramolecular protonation and k_{ext} is the rate constant for formation of product derived from external protonation, then the two rates for formation of internal protonation product and external protonation product, are given, respectively, as in eqs 3a and 3b where *n* and *m* are the number of HA molecules involved in each transition state. This leads to eq 4.

$$P_{int} = k_{int}[HA]^n[enolate] \quad (3a)$$

$$P_{ext} = k_{ext}[HA]^m[enolate] \quad (3b)$$

$$\log(P_{int}/P_{ext}) = (n - m)\log[HA] + \log(k_{int}/k_{ext}) \quad (4)$$

Hence the plot of the log of the product ratio affords a linear plot as obtained above in Figure 3, with a slope of $(n - m)$. The slope corresponds to the difference in the number of acid molecules involved in internal relative to external protonation. In the present case of ketonization of the amino enolate of silyl enol ether **24** this value (0.93) is within experimental error of unity. The intercept, here 1.25, gives the log of the ratio of the rate constants or a ca. 17-fold more rapid intramolecular rate relative to the intermolecular one.

Computational Counterpart. The stereochemistry of kinetic protonation has not been the subject of computational analysis. Nevertheless, this approach promised to shed light on the experimental results we observed and which are described above. Most promising were QST3 and IRC treatments. QST3 methodology starts with a reactant, a product, and an approximation for that transition structure and leads to an optimized final transition state structure. IRC computations provide a pathway for a reaction. Both approaches are available in the Gaussian programming suite.[8]

Computations were carried out on the reactions of the carboxylic acid **25** and on the aminomethylene relative **26**. For simplicity these molecular species of interest were truncated with a formyl group replacing benzoyl and formic acid replacing the acetic acid proton source. We designate these truncated species with an added "**T**". Computations were carried out on the reactant enolates, the ketonized products and also a transition structure which resulted in one case. Two types of computation were run, QST3 and IRC. For the QST3 runs, a basis of RHF/3-21g was employed. Density functional B3lyp/6-31+G(d) was used to assess the energy of each geometry optimized species. For the IRC and Frequency computations the RHF/3-21g was also used.[9] The choice of computational methodology was based

(8) (a) Frisch, M. J.; Trucks, G. W.; Schlegel, H. B.; Scuseria, G. E.; Robb, M. A.; Cheeseman, J. R.; Zakrzewski, V. G.; Montgomery, J. A., Jr.; Stratmann, R. E.; Burant, J. C.; Millam, J. M.; Daniels, A. D.; Kudin, K. N.; Strain, M. C.; Farkas, O.; Tomasi, J.; Barone, V.; Cossi, M.; Cammi, R.; Mennucci, B.; Pomelli, C.; Adamo, C.; Clifford, C.; Ochterski, J.; Petersson, G. A.; Ayala, P. Y.; Cui, Q.; Morokuma, K.; Malick, D. K.; Rabuck, A. D.; Raghavachari, K.; Foresman, J. B.; Cioslowski, J.; Ortiz, J. V.; Stefanov, B. B.; Liu, G.; Liashenko, A.; Piskorz, P.; Komaromi, I.; Gomperts, R.; Martin, R. L.; Fox, D. J.; Keith, T.; Al-Laham, M. A.; Peng, C. Y.; Nanayakkara, A.; Gonzalez, C.; Challacombe, M.; Gill, P. M. W.; Johnson, B.; Chen, W.; Wong, M. W.; Andres, J. L.; Gonzalez, C.; Head-Gordon, M.; Replogle, E. S.; Pople, J. A. *Gaussian 98*, Revision A.9; Gaussian, Inc.: Pittsburgh, PA, 1998.

(9) The size of the molecular systems studied, their considerable number, and the number of points needed in some of the computations necessitated a compromise in choice of the quantum mechanical method and basis set used. Those selected represent a practical and respectable choice leading to more than qualitative results.

SCHEME 5. QST3 Computation[a]

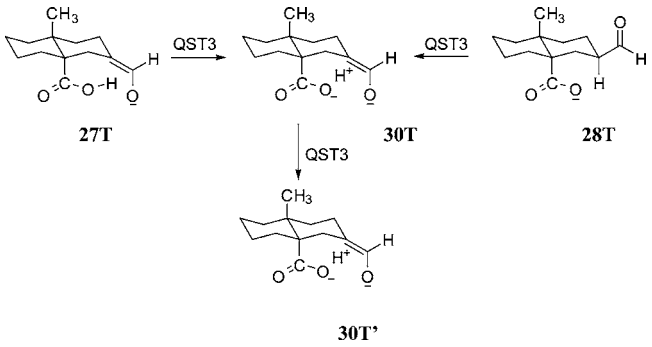

[a] The prime signifies the optimized species.

SCHEME 6. IRC Computational Results

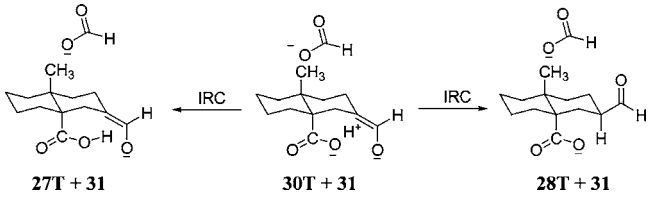

on practicality and for quantitative and meaningful but approximate aims.

We now turn now to a QST3 computation with the carboxylic acid enolate **27T** and product **28T** structures being introduced. However, in this case, a guess at a transition structure **30T** was also required. A reasonable choice placed the proton from these species geometrically halfway between the carboxylate oxygen and the α-carbon of the enolate. It was found that for success it was necessary to introduced one formate molecule **31**, this simulating an acetate species.

Interestingly, the formate anion moved in the transition state obtained to the reverse face of the decalin moiety; note Scheme 5. The transition state was checked with a frequency computation, which showed one imaginary frequency suggesting the species obtained to be the desired transition state.

IRC computations (RHF/3-21G) were carried out on species **27T**, **30T**, and **28T** along with the accompanying formate anion **31** in each case. The transition state, **30T**+**31**, was taken from the QST3 results and followed onward to reactant and product. In one direction, the computation gave the carboxylic acid-enolate **27T** with formate again at the backside of the decalin structure. In the other direction the IRC computations gave the product formyl carboxylate **28T**, again with a backside formate.

These computations are outlined in Scheme 6. Thus, as a consequence of microscopic reversibility, the pathway from compound **27T** to product **28T** was obtained. The b3lyp computations on **27T**, **30T**, and **28T** afforded the activation energies in both directions. The energy difference between starting carboxylic-enolate **27T** and the transition state **30T** is very small ($\Delta E = 0.44$ kcal/mol), whereas the energy difference between the transition state **30T** and the ketonized product **28T** is relatively large ($\Delta E = 9.98$ kcal/mol) (note Figure 4).

QST3 computations with the amino derivative were carried out. The transition state showed the proton located between the amino group and the enolate α-carbon (Scheme 7), and the frequency computation confirmed that it is a transition state with one imaginary frequency. An IRC computation of the reaction pathway from compound **32T** to compound **33T** was also carried out. Starting with **34T′** in the reverse direction am-

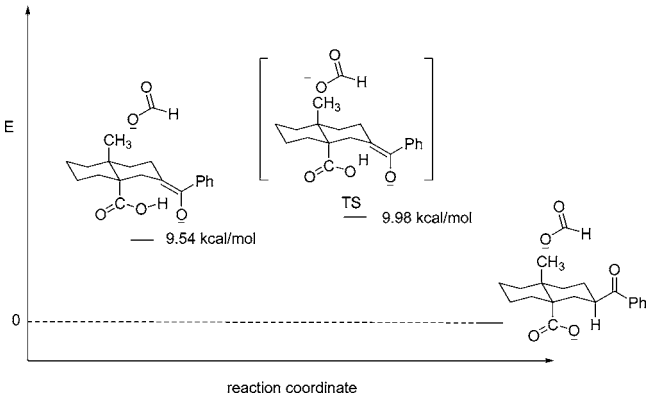

FIGURE 4. Energies for proton transfer with carboxyl.

SCHEME 7. QST3 Transition State Determination[a]

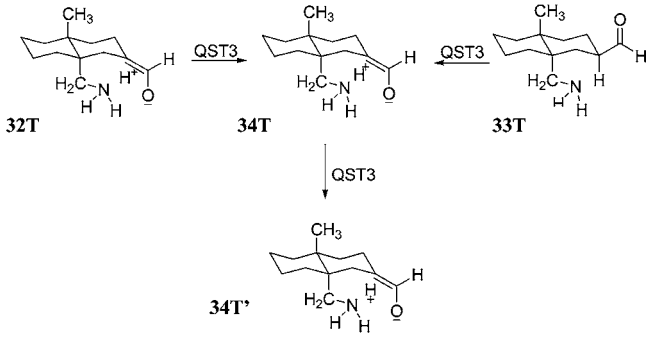

[a] The prime signifies the optimized species.

SCHEME 8. IRC Determination of Transition State

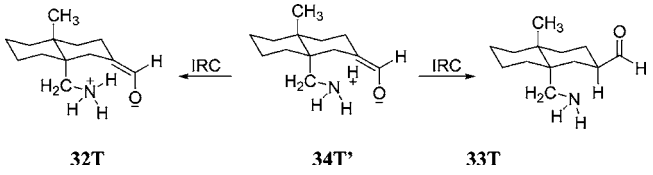

monium enolate, reactant **32T** resulted. In the other direction the product formyl amino derivative **33T** resulted (Scheme 8).

A B3lyp/6-31+G(d)) computation on species **32T**, **34T**, and **33T** revealed the activation energies in both directions. The energy difference between starting species and the transition state is very small ($\Delta E = 0.41$ kcal/mol), whereas the energy difference between the transition state and the product species is relatively large ($\Delta E = 31$ kcal/mol). See Figure 5.

Discussion

Qualitative Ketonization. The first noteworthy point is that the stereochemistry of kinetic protonation conforms to expectation of least hindered attack in those cases where the potentially internal transferring group is insufficiently basic as in the hydroxymethylene, the methoxymethoxymethylene, and the carboxaldehyde examples. A second point is that the computational results provide more than qualitative evidence for the close to sp^2 hybridization of the α-carbon in the transition state. The two examples of intramolecular proton transfer with carboxyl and ammonium moieties, are particularly instructive. Thus, the QST3 optimized transition structures with their imaginary frequencies have geometries which are nearly planar. Note Figure 6a and b.

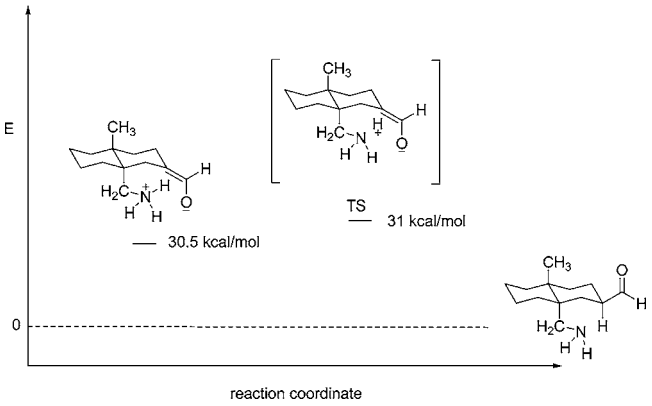

FIGURE 5. Reaction energetics for the aminomethylene case.

Of particular interest is the hybridization that is obtainable from the three valence angles. The first clue comes from the sum of the three interorbital angles *adb*, *adc*, and *bdc*. Note Figure 7. In the carboxylic acid transition structure these totaled 350.5° and 358.9° in the case of the aminomethylene transition structure. If these transition structures were exactly sp^2 hybridized, the sum would of course be 360°. A second approach was placement, using the Gausview program, of a phantom atom *P* equidistant from atoms *a* and *b*. The angle *Pdc* obtained in the carboxylic acid case was 150° and in the aminomethylene case was 168.7°. With perfect sp^2 hybridization an angle of 180° would have resulted. In both cases the deviation led to the enolate carbon moving upward (note the various drawings).

A more precise measurement of hybridization was obtained by vector analysis predicated on the three valence angles *adb*, *adc*, and *bdc* of the three σ hybrid orbitals. In the carboxylic acid transition structure the hybridization of the internal sigma bonds is designated $sp^{2.36}$, and $sp^{2.09}$ for the exocyclic σ bond. For the aminomethylene transition structure the endocyclic hybrids were $sp^{2.33}$ and the exocyclic bond was $sp^{2.04}$. Details of the method are given in Supporting Material and the general treatment of hybrids may be found in ref 10. The net result is that the transition structures are, indeed, very close to sp^2 hybridized and constitute "early" as surmised from the considerable exothermicity of the ketonization process.

Additionally, the ketonization process is highly exothermic as seen in Figures 4 and 5 where proton transfer is exothermic by 9.5 and 30.5 kcal/mol for the carboxyl and amino reactions. Equally interesting is the very minor activation energies for proton transfer (i.e. 0.4 and 0.5 kcal/mol, respectively).

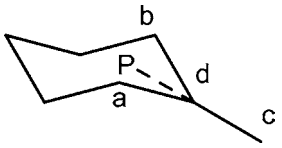

FIGURE 7. Vector analysis definitions.

Solvent and Buffer Effects. One intriguing result is provided by the lithium acetate/acetic acid buffered runs in DMSO in the carboxylic acid case. The lithium acetate concentration had been varied from 0.1 to 1.8 M, and the ratio of acetate to acetic acid then varied from 0.5:1 to 8:1. In the DMSO conditions, the carboxyl group of the carboxylic enolate **26** must be very heavily ionized. However, this moiety still is capable of transferring the proton intramolecularly by rapidly reversible but endothermic proton transfer. In THF one observes the same intramolecular transfer. Hence the carboxylate moiety is nevertheless capable of picking up a proton and transferring it to the α-carbon of the enolate group.

Significance of the Kinetics. It is noted above that the plot of the log of the product ratio P_{intra}/P_{inter} versus the log of acetic acid in the amino-decalyl enol reactions leads to a slope and an intercept of special interest. Thus the slope, $n - m$, affords the difference in acetic acid concentration in the intermolecular relative to the intramolecular protonation. The very close to unity slope indicates that two acetic acid molecules are involved in the intramolecular process if we assume that a single acetic acid molecule is needed for intermolecular protonation of the enolate α-carbon. If it were an acetic acid dimer that did the external protonation, there would be three acetic acid molecules in the intramolecular transfer. The computations were made assuming a single molecule for external attack. This did lead to a valid computational transition structure. The interesting involvement of two acetic acid molecules has precedent in our previous studies.[5,6] The simplest rationale is that intramolecular protonation involves an acetic acid dimer whereas external protonation does not. A variation is that the acetate species developing in the protonation process deprotonates a second acetic acid molecule which, in turn, converts the enol oxygen to enolate. This sequence then leads to protonation of an enolate moiety rather than the original enol. It is well-known that enolates α-protonate more readily than the neutral counterparts.

One point requiring explanation is the necessity of introduction of the formate anion in the computations. A general weakness of "gas-phase" computations is that these often are unrelated to the experimental conditions. The introduction of a

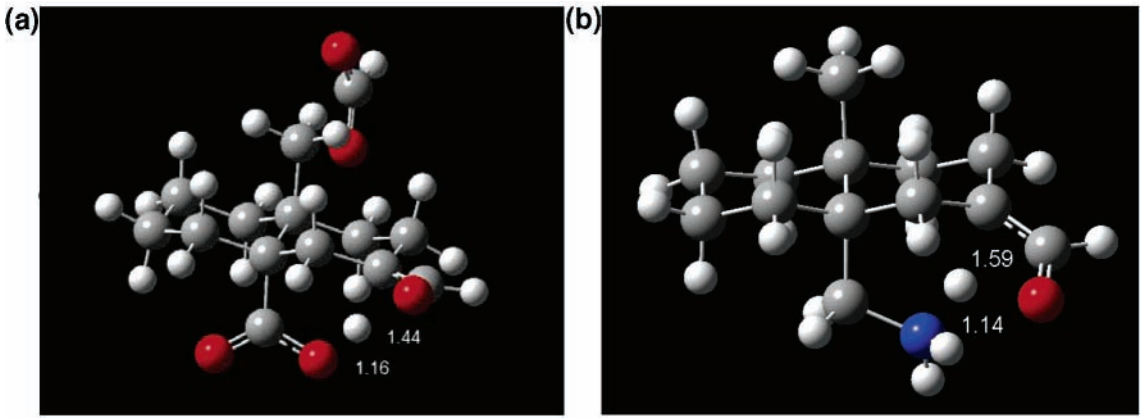

FIGURE 6. Transition structures for the carboxylic acid and aminomethylene cases.

single formate anion provides a basic neighbor thus emulating to some extent the experimental conditions. Although two acetic acid molecules are experimentally involved, computationally one seems sufficient. In the QST3 computations, using Gaussview, it was possible to inspect the geometry of the rearranging species early and before the transition structure. This revealed the formate molecule to be close to the proton being transferred in both the carboxylic acid and aminomethylene cases. However, as the reaction proceeded toward the transition structure, the formate molecule moved to the top of the decalyl system (note Scheme 5). In the aminomethylene example, the formate species followed close to the proton being transferred to the α-carbon as the reaction proceeded. However, in this latter case, QST3 was not successful and an amino-enolate-formate complex was produced. However, without formate the computation led nicely to the transition structure. The need in the QST3 computations for the formate anion for the carboxyl reactivity but not for the aminomethylene counterpart seems to arise from keeping the proton from bonding too readily to the α-carbon with a carboxylate present.

We note the sharp contrast between the aminodecalyl enol with the carboxyl enol wherein no acid dependence was encountered in the latter case. This seems most likely to arise from the much lower basicity of the carboxyl function as the transferring group compared with aminomethylene. Thus appreciable reversible protonation of the amino function and lack thereof in the carboxyl case is not unexpected. This conclusion is confirmed by the behavior in the aminomethylene example when phenol is the source of the proton. Phenol protonates intermolecularly with formation of the axial keto moiety as a consequence of the inability of phenol to provide a proton to the aminomethylene group. We do note that in the aminodecalyl system one does find appreciable external protonation 1:1; this occurs with the lowest acetic acid concentration of 0.05 M.

Conclusion. The stereochemistry of kinetic protonation of mesomeric species has a long history. Remarkably, the early qualitative interpretation has proven valid.

Experimental Section

General Procedures. Column chromatography (CC) was performed on silica gel (silica gel 35−75 μm or 60−200 mesh) mixed with 1% (v/v) of phosphor green UV254 fluorescent indicator and slurry packed into quartz columns to allow monitoring with a handheld UV lamp. All solvents were freshly distilled under a nitrogen atmosphere, from the appropriate drying agent before use.

(*Z*)-3-Benzylidene-*trans*-8a-methyl-octahydro-naphthalene-4a-carbonitrile (3) and (*E*)-3-Benzylidene-*trans*-8a-methyl-octahydro-naphthalene-4a-carbonitrile (4). To a stirred solution of potassium *tert*-butoxide (560 mg, 5.0 mmol) in 10 mL of *tert*-butyl alcohol was added a solution of benzyltriphenylphosphonium chloride (1.94 g, 5.0 mmol) in 10 mL of anhydrous *tert*-butyl alcohol. The mixture was stirred for 10 min and turned yellow. A solution of *trans*-9-methyl-10-cyanodecalone-3 (**2**) (960 mg, 5.0 mmol) in 10 mL of *tert*-butyl alcohol was added into the mixture dropwise. The mixture was stirred for 14 h. After TLC indicated the starting material was consumed, the mixture was diluted with water and hexane extracted. The combined solvents were dried (Na_2SO_4) and concentrated in vacuo. The residue was subjected to column chromatography to give 856 mg (67%) of a mixture of (*Z*)-3-benzylidene-*trans*-8a-methyl-octahydro-naphthalene-4a-carbonitrile (**3**) and (*E*)-3-benzylidene-*trans*-8a-methyl-octahydro-naphthalene-4a-carbonitrile (**4**). Crystallization from hexanes−ether gave 400 mg of (*Z*)-3-benzylidene-*trans*-8a-methyl-octahydro-naphthalene-4a-carbonitrile (**3**) as colorless crystals: mp 127−129 °C; ^{1}H NMR (500 MHz, $CDCl_3$) δ 7.35−7.32 (m, 2H), 7.27−7.25 (m, 2H), 7.24−7.21 (m, 1H), 6.53 (s, 1H), 2.77 (d, J = 14 Hz, 1H), 2.61−2.54 (m, 1H), 2.38−2.34 (m, 1H), 2.12 (dt, J = 14.5, 1.8 Hz, 1H), 1.85 (td, J = 13.8, 5 Hz, 1H), 1.81−1.71 (m, 2H), 1.70−1.60 (m, 3H), 1.58−1.54 (m, 2H), 1.47 (ddd, J = 13.5, 5.5, 2 Hz, 1H), 1.40−1.37 (m, 1H), 1.11 (s, 3H); ^{13}C NMR (75 MHz, $CDCl_3$) δ 137.5, 136.5, 129.2, 128.3 (2), 127.1 (2), 126.5, 123.1, 46.6, 38.7, 37.2, 35.9, 34.9, 31.6, 31.4, 23.0, 20.6, 16.5; HRMS-EI m/z (M^+) calcd for $C_{19}H_{23}N$ 265.1830, found 265.1839.

Further concentration of the mother liquid gave 300 mg of (*E*)-3-benzylidene-*trans*-8a-methyl-octahydro-naphthalene-4a-carbonitrile (**4**) as colorless crystals: mp 96−98 °C; ^{1}H NMR (500 MHz, $CDCl_3$) δ 7.31−7.28 (m, 2H), 7.23−7.21 (m, 2H), 7.20−7.16 (m, 1H), 6.40 (s, 1H), 2.81−2.77 (m, 1H), 2.48 (dt, J = 13.5, 1.8 Hz, 1H), 2.25−2.18 (m, 2H), 1.83−1.73 (m, 2H), 1.66−1.57 (m, 6H), 1.36−1.31 (m, 2H), 1.09 (s, 3H); ^{13}C NMR (75 MHz, $CDCl_3$) δ 137.2, 136.3, 128.8 (2), 127.8 (2), 126.7, 126.1, 122.6, 47.0, 42.2, 37.8, 36.8, 35.3, 31.0, 24.0, 22.7, 20.2, 16.2; HRMS-EI m/z (M^+) calcd for $C_{19}H_{23}N$ 265.1830, found 265.1838.

(*Z*)-3-Benzylidene-*trans*-8a-methyl-octahydro-naphthalene-4a-carboxaldehyde (5). To an ether solution (8.0 mL) of (*Z*)-3-benzylidene-*trans*-8a-methyl-octahydro-naphthalene-4a-carbonitrile (**3**) (265.4 mg, 1.0 mmol) was added diisobutylaluminum hydride (1.5 mL, 1.0 M in hexane, 1.5 equiv) at 0 °C. After the mixture was stirred at 0 °C for 1 h, 5.0 mL of 6% acetic acid saturated with sodium acetate was added along with 5.0 mL of THF to dissolve the white precipitate. The aqueous layer was ether extracted. The combined extracts were washed with saturated $NaHCO_3$ solution. The aqueous layer was then ether extracted. The solvents were combined, washed with brine, and dried (Na_2SO_4). Removal of the solvent in vacuo and subsequent column chromatography afforded aldehyde **5** (231 mg, 86%) as a white solid: mp 78−80 °C; ^{1}H NMR (300 MHz, $CDCl_3$) δ 9.44 (s, 1H), 7.32−7.26 (m, 2H), 7.20−7.17 (m, 1H), 7.15−7.12 (m, 2H), 6.30 (s, 1H), 2.69−2.57 (m, 2H), 2.28 (dd, J = 15, 5.4 Hz, 1H), 2.19−2.07 (m, 2H), 1.88 (td, J = 13, 4.8 Hz, 1H), 1.70−1.59 (m, 1H), 1.57−1.51 (m, 2H), 1.48 (d, J = 3 Hz, 1H), 1.45 (d, J = 3.3 Hz, 1H), 1.32 (ddd, J = 13.2, 6, 1.8 Hz, 1H), 1.25−1.19 (m, 2H), 1.17 (s, 3H); ^{13}C NMR (75 MHz, $CDCl_3$) δ 206.9, 137.7, 137.3, 128.7 (2), 127.9 (2), 126.0, 124.9, 54.0, 35.8, 35.3, 35.2, 34.0, 32.3, 29.2, 22.5, 21.0, 20.5; HRMS-EI m/z (M^+) calcd for $C_{19}H_{24}O$ 268.1827, found 268.1837.

(*Z*)-3-Benzylidene-4a-hydroxymethylene-*trans*-8a-methyl-octahydro-naphthalene (6). The (*Z*)-3-benzylidene-*trans*-8a-methyl-octahydro-naphthalene-4a-carboxaldehyde (**5**) (180 mg, 0.67 mmol) was dissolved in 3.0 mL of anhydrous THF and cooled to −78 °C. Diisobutylaluminum hydride (1.0 mL, 1.0 M in hexane, 1.5 equiv) was added at −78 °C and the mixture was stirred for 1 h. TLC indicated the comsumption of the starting material. The solution was diluted with 3.0 mL of ether, and 1.0 mL of water was added dropwise at 0 °C. Then 3.0 mL of 1 N HCl was added and stirred for 5 min. The water layer was ether extracted, and the extracts were washed with saturated sodium bicarbonate solution. This aqueous layer was then extracted with ether. The combined solvents were washed with brine, and dried (Na_2SO_4). Removal of the solvent in vacuo and column chromatography (hexane/ether, 5:1) afforded **6** (104 mg, 57%) as a white solid: mp 112−114 °C; ^{1}H NMR (300 MHz, $CDCl_3$) δ 7.32−7.27 (m, 2H), 7.23−7.15 (m, 3H), 6.37 (s, 1H), 3.76 (dd, J = 11.4, 1.8 Hz, 1H), 3.67 (d, J = 11.2 Hz, 1H), 2.70−2.60 (m, 1H), 2.55 (dd, J = 14.4, 1.2 Hz, 1H), 2.25 (dd, J = 15.2, 5.2 Hz, 1H), 1.90 (dd, J = 14.8, 1.8 Hz, 1H), 1.69−1.37 (m, 7H), 1.29−1.20 (m, 1H), 1.18 (s, 3H), 1.16−0.88 (m, 2H); ^{13}C NMR (75 MHz, $CDCl_3$) δ 140.5, 138.1, 129.2 (2), 128.1 (2), 126.0, 125.0, 60.8, 41.3, 40.4, 35.4, 35.1, 34.4, 27.0,

(10) (a) Paufler, R.; Zimmerman, H. E. Unpublished results. Paufler, R. Ph.D. Dissertation. Ketonization of a Dienol and the Synthesis of Bicyclo-[2.2.2]-Octatriene (Barrelene). Northwestern University, 1960; p 16. (b) Malhotra, S. K.; Ringold, H. *J. Am. Chem. Soc*. **1965**, *87*, 3228−3226.

(11) *Quantum Mechanics for Organic Chemists*; Zimmerman, H. E.; Academic Press: New York, 1975.

24.7, 21.1, 21.0, 20.5; HRMS-EI *m*/*z* (M^+) calcd for $C_{19}H_{26}O$ 270.1984, found 270.1992.

3-*endo*-(1-Hydroxybenzyl)-4a-hydroxymethylene-*trans*-8a-methyl-decahydro-naphthalene (7). A solution of 96 mg (0.35 mmol) of (*Z*)-3-benzylidene-4a-hydroxymethylene-*trans*-8a-methyl-octahydro-naphthalene (**6**) in 2.8 mL of 1.0 M borane in THF was stirred at ambient temperature for 20 h. The mixture was cooled with an ice bath, 95% ethanol was added to quench the remaining borane, and a solution of 227 mg (5.68 mmol) of sodium hydroxide solution in 4.0 mL of water and then 2.1 mL of 30% hydrogen peroxide (21.3 mmol) were added slowly with stirring. After being stirred for 2 h at room temperature, the mixture was poured into 15 mL of saturated ammonium chloride solution and the aqueous solution was ether extracted. The combined extracts were washed with brine, dried (Na_2SO_4), and concentrated in vacuo. The residue was chromatographed on a silica gel column (hexane/ether, 1:1) to give 80 mg (87%) of **7**: mp 86−87 °C; ^{1}H NMR (300 MHz, $CDCl_3$) δ 7.29−7.26 (m, 4H), 7.25−7.20 (m, 1H), 4.59 (d, J = 5.4 Hz, 1H), 3.85 (dd, J = 11.7, 0.9 Hz, 1H), 3.61 (dd, J = 11.4, 0.9 Hz, 1H), 3.13 (brs, 2H), 2.25−2.15 (m, 1H), 1.82−1.68 (m, 1H), 1.54−1.30 (m, 8H), 1.27−1.17 (m, 2H), 1.14−1.04 (m, 3H), 0.98 (s, 3H); ^{13}C NMR (75 MHz, $CDCl_3$) δ 143.6, 128.0 (2), 127.0, 126.2 (2), 78.0, 62.3, 39.5, 37.1, 35.7, 34.1, 33.2, 30.6, 29.5, 23.8, 21.1, 20.9, 18.0; HRMS-EI *m*/*z* ([M − H_2O]$^+$) calcd for $C_{19}H_{26}O$ 270.1984, found 270.1980.

3-*endo*-Benzoyl-decahydro-*trans*-8a-methyl-naphthalene-4a-carboxaldehyde (8). To oxalyl chloride (33 μL, 0.38 mmol) in 2.0 mL of CH_2Cl_2 at −78 °C was added dropwise DMSO (71 μL, 0.83 mmol). The mixture was stirred at −78 °C for 3 min followed by the addition of the solution of 3-*endo*-(1-hydroxybenzyl)-4a-hydroxymethylene-*trans*-8a-methyl-decahydro-naphthalene (**7**) (50 mg, 0.17 mmol) in 0.5 mL of CH_2Cl_2. Triethylamine (241 μL, 1.73 mmol) was added after the mixture was stirred for 20 min. The reaction mixture was stirred for 10 min followed by warming to room temperature. The mixture was diluted with water and CH_2Cl_2 extracted. The combined extracts were washed with brine, dried (Na_2SO_4), and concentrated in vacuo. Crystallization of the crude product gave 45 mg (91%) of **8** as white crystals: mp 94−96 °C; ^{1}H NMR (300 MHz, $CDCl_3$) δ 9.91 (s, 1H), 7.8−7.77 (m, 2H), 7.55−7.49 (m, 1H), 7.46−7.40 (m, 2H), 3.54 (tt, J = 7.2, 2.1 Hz, 1H), 2.22 (td, J = 13, 5.6 Hz, 1H), 2.05−1.82 (m, 5H), 1.76−1.59 (m, 1H), 1.57−1.37 (m, 4H), 1.34−1.13 (m, 3H), 1.12 (s, 3H); ^{13}C NMR (75 MHz, $CDCl_3$) δ 208.8, 204.9, 136.4, 132.6, 128.6 (2), 128.5 (2), 51.1, 39.2, 34.5, 34.1, 32.5, 32.4, 31.6, 22.3, 20.9, 20.8, 20.0; HRMS-EI *m*/*z* ([M − CO]$^+$) calcd for $C_{18}H_{24}O$ 256.1827, found 256.1817.

3-*endo*-Benzoyl-decahydro-*trans*-8a-methyl-naphthalene-4a-carboxylic Acid (9). To a solution of 3-*endo*-benzoyl-decahydro-*trans*-8a-methyl-naphthalene-4a-carboxaldehyde (**8**) (493 mg, 1.73 mmol) in 50 mL of acetone at 0 °C was slowly added 4.0 mL of Jones reagent (2.84 M). The reaction mixture was stirred for 30 min. A lot of green solid precipitated. Then 1.0 mL of isopropyl alcohol was added to destroy excess chromium oxidant. The mixture was diluted with water and ether extracted. The combined solvents were washed with brine, dried over sodium sulfate, and concentrated in vacuo. The residue was subjected to column chromatography (hexane/ether, 3:1) to give 396 mg (76%) of **9** as a white solid: mp 198−200 °C; ^{1}H NMR (300 MHz, CD_3COCD_3) δ 7.90−7.87 (m, 2H), 7.56−7.51 (m, 1H), 7.47−7.42 (m, 2H), 3.74−3.71 (m, 1H), 2.57−2.49 (m, 2H), 2.34 (d, J = 14.4 Hz, 1H), 2.15−2.06 (m, 1H), 1.98−1.90 (m, 2H), 1.74−1.59 (m, 1H), 1.53−1.41 (m, 4H), 1.34−1.21 (m, 1H), 1.14 (s, 3H), 1.07−0.94 (m, 2H); ^{13}C NMR (75 MHz, CD_3COCD_3) δ 204.0, 176.7, 138.5, 133.2, 129.7 (2), 129.6 (2), 49.2, 40.7, 36.4, 35.6, 34.3, 33.9, 30.4, 23.7, 22.4, 22.1, 22.0; HRMS-EI *m*/*z* (M^+) calcd for $C_{19}H_{24}O_3$ 300.1725, found 300.1725.

(*Z*)-3-((*tert*-Butyldimethylsilyloxy)(phenyl)methylidene)-*trans*-8a-methyl-octahydro-naphthalene-4a-carboxylic Acid *tert*-Butyldimethylsilyl Ester (10). To a solution of diisopropylamine (93 μL, 0.67 mmol) in 3.0 mL of THF was added 0.24 mL of *n*-BuLi (2.8 M, 0.67 mmol) under nitrogen at −78 °C. The reaction mixture was stirred for 30 min and HMPA (0.23 mL, 1.33 mmol) was added and stirred for 15 min. Then 1.0 mL of a THF solution of 3-*endo*-benzoyl-decahydro-*trans*-8a-methyl-naphthalene-4a-carboxylic acid (**9**) (50 mg, 0.17 mmol) was slowly added and stirred for 20 min, followed by 1.0 mL of THF solution of TBSCl (100 mg, 0.67 mmol). The reaction temperature was allowed to gradually reach room temperature overnight and was quenched with water. The mixture solution was extracted with ether. The combined solvents were washed with water and brine, dried over sodium sulfate, and concentrated in vacuo to give the crude material, which was subjected to column chromatography (hexane/ether, 160:1) to give 48 mg (55%) of **10** as white crystals: mp 74−76 °C; ^{1}H NMR (300 MHz, $CDCl_3$) δ 7.23−7.16 (m, 5H), 3.11 (d, J = 15 Hz, 1H), 2.31−2.23 (m, 3H), 1.95 (d, J = 15 Hz, 1H), 1.90−1.80 (m, 2H), 1.58−1.49 (m, 5H), 1.28−1.20 (m, 2H), 1.08 (s, 3H), 0.93 (s, 9H), 0.77 (s, 9H), 0.28 (s, 3H), 0.27 (s, 3H), −0.14 (s, 3H), −0.30 (s, 3H); ^{13}C NMR (75 MHz, $CDCl_3$) δ 176.3, 143.4, 139.3, 129.6 (2), 127.7 (2), 116.0, 52.3, 35.7, 35.3, 32.5, 26.2, 26.1, 25.9, 24.5, 23.7, 21.4, 21.3, 18.6, 18.1, −3.8, −4.1, −4.4, −4.5; HRMS-EI *m*/*z* ([M − H_2O]$^+$) calcd for $C_{31}H_{52}O_3Si_2$ 528.3455, found 528.3439.

(*Z*)-3-((*tert*-Butyldimethylsilyloxy)(phenyl)methylidene)-*trans*-8a-methyl-octahydro-naphthalene-4a-carboxylic Acid (11). To a solution of (*Z*)-3-((*tert*-butyldimethylsilyloxy)(phenyl)methylidene)-*trans*-8a-methyl-octahydro-naphthalene-4a-carboxylic acid *tert*-butyldimethylsilyl ester (**10**) (53 mg, 0.1 mmol) in 2.0 mL of methanol and 0.5 mL of tetrahydrofuran was added a solution of 48 mg of potassium carbonate in 0.7 mL of water. The reaction mixture was stirred at 25 °C for 10 min and diluted with 3.0 mL of water. The aqueous mixture was cooled to 0 °C, adjusted to pH 2−3 with 1.0 N hydrochloric acid, and hexane extracted. The combined extracts were washed with brine, dried over sodium sulfate, and concentrated in vacuo to give the crude material, which was subjected to column chromatography (hexane/ether, 20:1) to give 38 mg (93%) of **11** as white crystals: mp 149−151 °C; ^{1}H NMR (300 MHz, $CDCl_3$) δ 7.25−7.22 (m, 3H), 7.21−7.17 (m, 2H), 3.22 (d, J = 13.8 Hz, 1H), 2.25−2.07 (m, 3H), 2.0 (d, J = 14.1 Hz, 1H), 1.92−1.86 (m, 1H), 1.69−1.57 (m, 3H), 1.52−1.44 (m, 1H), 1.41−1.33 (m, 1H), 1.11 (s, 3H), 1.07−0.92 (m, 3H), 0.86 (s, 9H), −0.18 (s, 3H), −0.38 (s, 3H); ^{13}C NMR (75 MHz, $CDCl_3$) δ 181.4, 139.0, 129.8, 127.9 (2), 127.5 (2), 126.8, 115.7, 55.5, 36.1, 36.0, 35.1, 33.4, 31.8, 26.1, 26.0, 25.9, 25.0, 23.7, 21.3, 21.2, 18.4, −4.0, −4.1; HRMS-EI *m*/*z* (M^+) calcd for $C_{25}H_{38}O_3Si$ 414.2590, found 414.2600.

(*Z*)-3-Benzylidene-4a-methoxymethoxymethylene-*trans*-8a-methyl-octahydro-naphthalene (12). To the stirred solution of **6** (140 mg, 0.52 mmol) in 3.5 mL of dimethoxymethane were added 15 mg of lithium bromide and 10 mg of *p*-toluenesulfonic acid at room temperature and the mixture was continuously stirred for 24 h. The mixture was diluted with 10 mL of saturated sodium chloride solution and ether extracted. The combined solvents were washed with brine, dried over sodium sulfate, and concentrated in vacuo to give the crude material, which was subjected to column chromatography (hexane/ether, 80:1) to give 128 mg (79%) of **12** as colorless solid: mp 116−118 °C; ^{1}H NMR (300 MHz, $CDCl_3$) δ 7.27−7.18 (m, 4H), 7.14−7.09 (m, 1H), 6.34 (s, 1H), 4.26 (d, J = 6.9 Hz, 1H), 4.18 (d, J = 6.3 Hz, 1H), 3.79 (dd, J = 9.6, 2 Hz, 1H), 3.37 (dd, J = 9.3, 0.6 Hz, 1H), 3.05 (s, 3H), 2.80 (d, J = 13.8 Hz, 1H), 2.70−2.61 (m, 1H), 2.25 (dd, J = 15.6, 5.1 Hz, 1H), 1.92 (dd, J = 14.4, 1.8 Hz, 1H), 1.71−1.38 (m, 6H), 1.34−1.21 (m, 2H), 1.18 (s, 3H), 1.15−1.03 (m, 2H); ^{13}C NMR (75 MHz, $CDCl_3$) δ 140.4, 138.5, 129.2 (2), 128.2 (2), 126.0, 125.4, 97.3, 66.6, 55.3, 40.9, 40.8, 35.5, 35.3, 34.7, 27.7, 24.7, 21.2, 21.1, 20.2; HRMS-EI *m*/*z* (M^+) calcd for $C_{21}H_{30}O_2$ 314.2246, found 314.2234.

3-*endo*-Benzoyl-decahydro-4a-methoxymethoxymethylene-*trans*-8a-methyl-naphthalene (14). A solution of 125 mg (0.40 mmol) of (*Z*)-3-benzylidene-4a-methoxymethoxymethylene-*trans*-8a-methyl-octahydro-naphthalene (**12**) in 3.2 mL of 1.0 M borane

in THF was stirred at ambient temperature for 20 h. The mixture was cooled with an ice bath, 95% ethanol was added to quench the remaining borane, and a solution of 254 mg (6.36 mmol) of sodium hydroxide solution in 5.0 mL of water and then 2.4 mL of 30% hydrogen peroxide (23.8 mmol) were added slowly with stirring. After being stirred for 2 h at room temperature, the mixture was poured into 15 mL of saturated ammonium chloride solution and ether extracted. The combined extracts were washed with brine, dried over sodium sulfate, and concentrated in vacuo. The crude was used without further purification.

To oxalyl chloride (39 μL, 0.45 mmol) in 2.0 mL of CH_2Cl_2 at −78 °C was added dropwise DMSO (64 μL, 0.9 mmol). The mixture was stirred at −78 °C for 3 min followed by the addition of a solution of **13** (100 mg, 0.3 mmol) in 1.0 mL of CH_2Cl_2. Triethylamine (209 μL, 1.5 mmol) was added after the mixture was stirred for 20 min. The reaction mixture was stirred for 10 min followed by warming to room temperature. The mixture was diluted with water and CH_2Cl_2 extracted. The combined extracts were washed with brine, dried over sodium sulfate, and concentrated in vacuo. The residue was purified by column chromatography to give 84 mg (85%) of **14** as a white solid: mp 104−106 °C; ^{1}H NMR (300 MHz, $CDCl_3$) δ 7.88−7.84 (m, 2H), 7.51−7.45 (m, 1H), 7.42−7.36 (m, 2H), 4.27 (d, J = 6.6 Hz, 1H), 3.95 (d, J = 6.6 Hz, 1H), 3.88 (dd, J = 9.9, 1.2 Hz, 1H), 3.52 (t, J = 7.5 Hz, 1H), 3.35 (dd, J = 9.9, 1.2 Hz, 1H), 3.10 (s, 3H), 2.16−2.07 (m, 2H), 1.95−1.82 (m, 2H), 1.79−1.70 (m, 1H), 1.66−1.53 (m, 2H), 1.50−1.29 (m, 4H), 1.23−1.12 (m, 1H), 1.10 (s, 3H), 1.04−0.94 (m, 2H); ^{13}C NMR (75 MHz, $CDCl_3$) δ 205.8, 136.5, 132.4, 128.5 (2), 128.4 (2), 96.2, 64.5, 55.1, 39.4, 39.3, 34.8, 34.3, 32.8, 30.7, 28.5, 20.6, 20.3, 20.0, 19.8; HRMS-ESI m/z (MNa^+) calcd for $C_{21}H_{30}O_3Na$ 353.2093, found 353.2085.

(*Z*)-3-((*tert*-Butyldimethylsilyloxy)(phenyl)methylidene)-4a-methoxymethoxymethylene-*trans*-8a-methyl-octahydro-naphthalene (15). To a solution of diisopropylamine (53 μL, 0.38 mmol) in 2.0 mL of THF was added 0.17 mL of 2.2 M *n*-BuLi under nitrogen at −78 °C. The reaction mixture was stirred for 30 min and HMPA (0.13 mL, 0.75 mmol) was added and stirred for 15 min. Then a 1.0 mL of THF solution of 3-*endo*-benzoyl-decahydro-4a-methoxymethoxymethylene-*trans*-8a-methyl-naphthalene (**14**) (49 mg, 0.15 mmol) was slowly added and stirred for 20 min, followed by 0.5 mL of THF solution of TBSCl (57 mg, 0.38 mmol). The reaction temperature was allowed to gradually reach room temperature overnight and was quenched with water. The mixture solution was ether extracted. The combined solvents were washed with water and brine, dried over sodium sulfate, and concentrated in vacuo to give the crude material, which was subjected to column chromatography (hexane/ether, 40:1) to give 59 mg (88%) of **15** as a white solid: mp 55−57 °C; ^{1}H NMR (300 MHz, $CDCl_3$) δ 7.23−7.19 (m, 5H), 4.38 (d, J = 6.6 Hz, 1H), 4.22 (d, J = 6.3 Hz, 1H), 3.81 (dd, J = 9, 2.2 Hz, 1H), 3.38 (d, J = 9 Hz, 1H), 3.17 (s, 3H), 2.92 (dd, J = 15.6, 5.6 Hz, 1H), 2.25 (d, J = 14.7 Hz, 1H), 2.19−2.07 (m, 1H), 1.83 (d, J = 14.7 Hz, 1H), 1.67−1.58 (m, 1H), 1.50−1.33 (m, 6H), 1.20−1.14 (m, 1H), 1.12 (s, 3H), 1.07−0.94 (m, 2H), 0.85 (s, 9H), −0.14 (s, 3H), −0.30 (s, 3H); ^{13}C NMR (75 MHz, CD_2Cl_2) δ 144.4, 139.8, 129.9 (2), 128.0 (2), 127.5, 117.2, 97.6, 67.1, 55.4, 40.5, 35.4, 35.0, 33.5, 28.3, 26.2, 22.5, 21.7 (2), 20.1, 18.7, −4.0 (2); HRMS-EI m/z (M^+) calcd for $C_{27}H_{44}O_3Si$ 444.3060, found 444.3044.

(*Z*)-3-((*tert*-Butyldimethylsilyloxy)(phenyl)methylidene)-*trans*-8a-methyl-octahydro-naphthalene-4a-carboxaldehyde (16) and (*E*)-3-((*tert*-Butyldimethylsilyloxy)(phenyl)methylidene)-*trans*-8a-methyl-octahydro-naphthalene-4a-carboxaldehyde (17). To a solution of hexamethyldisilazane (556 μL, 2.64 mmol) in 10 mL of THF was added 1.2 mL of 2.2 M *n*-BuLi under nitrogen at −78 °C. The reaction mixture was stirred for 30 min and HMPA (0.92 mL, 5.28 mmol) was added and stirred for 15 min. Then 14 mL of a THF solution of 3-*endo*-benzoyl-decahydro-*trans*-8a-methyl-naphthalene-4a-carboxaldehyde (**8**) (500 mg, 1.76 mmol) was slowly added and stirred for 20 min, followed by 7.0 mL of THF solution of TBSCl (478 mg, 3.17 mmol). The reaction temperature was allowed to gradually reach room temperature for 3 h and was quenched with water. The mixture was hexane extracted, and the combined solvents were washed with water and brine, dried over sodium sulfate, and concentrated in vacuo to give the crude material, which was subjected to column chromatography (hexane/ether, 40:1) to give a mixture of *Z*- and *E*-isomers (617 mg, 88%). Crystallization from hexanes−ether gave 250 mg of *Z*-isomer **16**. The mother solution was concentrated and subjected to column chromatography (hexane/ether, 160:1) to give 160 mg of *Z*- isomer **16** and 200 mg of *E*-isomer **17**.

Spectrum data for 16: mp 74−76 °C; ^{1}H NMR (500 MHz, $CDCl_3$) δ 9.63 (s, 1H), 7.31−7.29 (m, 2H), 7.27−7.25 (m, 1H), 7.23−7.21 (m, 2H), 2.91 (d, J = 14.5 Hz, 1H), 2.28 (td, J = 14, 5 Hz, 1H), 1.92−1.80 (m, 2H), 1.70−1.63 (m, 1H), 1.61−1.55 (m, 3H), 1.53−1.48 (m, 1H), 1.31−1.23 (m, 1H), 1.13 (s, 3H), 1.11−1.06 (m, 2H), 0.89 (s, 9H), −0.15 (s, 3H), −0.31 (s, 3H); ^{13}C NMR (75 MHz, $CDCl_3$) δ 207.0, 143.7, 138.5, 129.6 (2), 127.9 (2), 127.6, 115.0, 54.0, 35.5, 35.2, 35.1, 31.5, 28.7, 26.0, 24.9, 22.5, 22.5, 21.0, 20.5, 18.4, −4.0, −4.1; HRMS-EI m/z (M^+) calcd for $C_{25}H_{38}O_2Si$ 398.2641, found 398.2660.

Spectrum data for 17: mp 70−72 °C; ^{1}H NMR (500 MHz, $CDCl_3$) δ 9.53 (s, 1H), 7.33−7.30 (m, 2H), 7.28−7.26 (m, 1H), 7.21−7.19 (m, 2H), 2.96 (dd, J = 15, 5 Hz, 1H), 2.21−2.14 (m, 2H), 2.07−1.99 (m, 2H), 1.83 (td, J = 13.5, 4 Hz, 1H), 1.68−1.57 (m, 1H), 1.50−1.48 (m, 2H), 1.43−1.27(m, 3H), 1.22−1.15 (m, 2H), 1.14 (s, 3H), 0.89 (s, 9H), −0.17 (s, 3H), −0.27 (s, 3H); ^{13}C NMR (75 MHz, $CDCl_3$) δ 208.2, 144.0, 138.7, 129.5 (2), 128.1 (2), 127.6, 115.0, 53.7, 35.3, 35.1, 34.7, 34.1, 29.0, 26.0, 22.5, 22.3, 21.0, 18.4, −4.2 (2); HRMS-EI m/z (M^+) calcd for $C_{25}H_{38}O_2Si$ 398.2641, found 398.2659.

(*Z*)-3-((*tert*-Butyldimethylsilyloxy)(phenyl)methylidene)-4a-hydroxymethylene-*trans*-8a-methyl-octahydro-naphthalene (18). (*Z*)-3-((*tert*-Butyldimethylsilyloxy)(phenyl)-methylidene)-*trans*-8a-methyl-octahydro-naphthalene-4a-carboxaldehyde (**16**) (100 mg, 0.25 mmol) was dissolved in 5.0 mL of anhydrous ether and cooled to −78 °C. Diisobutylaluminum hydride (0.25 mL, 1.5 M in toluene, 1.5 equiv) was added at −78 °C and the mixture was stirred for 1 h. TLC check indicated the comsumption of the starting material. The reaction mixture was warmed to room temperature. Then 1.0 mL of 6% acetic acid saturated with sodium acetate was added along with 1.5 mL of THF to dissolve the white precipitate. The solution was stirred for 10 min at room temperature. Then the mixture was diluted with water and hexane extracted. The combined solvents were washed with water and brine, dried (Na_2SO_4), and concentrated in vacuo to give the crude material, which was subjected to column chromatography (hexane/ether, 20:1) to give 94 (94%) mg of **18** as a white solid: mp 84−86 °C; ^{1}H NMR (300 MHz, $CDCl_3$) δ 7.31−7.24 (m, 5H), 3.83−3.71 (m, 2H), 2.63 (dd, J = 12.6, 1.2 Hz, 1H), 2.51 (brs, 1H), 2.31−2.18 (m, 2H), 1.73 (d, J = 14 Hz, 1H), 1.66−1.46 (m, 6H), 1.40−1.24 (m, 3H), 1.14 (m, 3H), 0.96−0.92 (m, 1H), 0.88 (s, 9H), −0.05 (s, 3H), −0.4 (s, 3H); ^{13}C NMR (75 MHz, $CDCl_3$) δ 142.9, 138.1, 129.7 (2), 128.0 (2), 127.7, 119.1, 61.9, 42.3, 36.1, 35.6, 34.6, 31.0, 27.1, 26.0, 25.6, 21.0, 20.8, 20.7, 18.3, −4.0, −4.5; HRMS-EI m/z (M^+) calcd for $C_{25}H_{40}O_2Si$ 400.2798, found 400.2790.

3-*endo*-Benzoyl-decahydro-4a-hydroxymethylene-*trans*-8a-methyl-naphthalene (19). A CH_2Cl_2 solution (1.0 mL) of TMSCl (12.3 μL, 0.1 mmol) was added to a stirred mixture of (*Z*)-3-((*tert*-butyldimethylsilyloxy)(phenyl)methylidene)-4a-methoxymethoxymethylene-*trans*-8a-methyl-octahydro-naphthalene (**15**) (40 mg, 0.09 mmol) and NaI (14.6 mg, 0.1 mmol) in CH_2Cl_2 solution (2.0 mL) and the mixture was kept at room temperature for 1 h. Then the mixture was diluted with water and CH_2Cl_2 extracted. The combined solvents were washed with water and brine, dried (Na_2SO_4), and concentrated in vacuo to give the crude material, which was subjected to column chromatography (hexane/ether, 5:1) to give 21 mg (83%) of **19** as a white solid: mp 155−157 °C; ^{1}H NMR (300 MHz, $CDCl_3$) δ 7.59−7.56 (m, 2H), 7.37−7.28 (m,

3H), 4.44 (dd, J = 11.7, 2.4 Hz, 1H), 3.79 (d, J = 11.7 Hz, 1H), 2.31 (brs, 1H), 2.13 (td, J = 13.2, 5.1 Hz, 1H), 2.05−2.01 (m, 1H), 1.96−1.90 (m, 1H), 1.84−1.42 (m, 7H), 1.23−1.09 (m, 2H), 1.04 (s, 3H), 1.02−0.83 (m, 3H); ^{13}C NMR (75 MHz, $CDCl_3$) δ 145.2, 128.2 (2), 127.9, 125.8 (2), 99.0, 68.8, 38.6, 36.0, 34.6, 34.4, 32.7, 30.7, 29.9, 23.4, 21.5, 21.1, 20.7; HRMS-EI $[M]^+$ (m/z) for $C_{19}H_{26}O_2$ calcd 286.1933; found 286.1931.

3-*endo*-Benzoyl-*trans*-8a-methyl-decahydro-naphthalene-4a-carbonitrile (22). To a solution of diisopropylamine (0.28 mL, 2 mmol) in 5.0 mL of THF was added 0.9 mL of 2.2 M *n*-BuLi under nitrogen at −78 °C. The reaction mixture was stirred for 30 min. Then 4.0 mL of THF solution of diethyl 1-methoxy-1-phenylmethylphosphonate (517 mg, 2 mmol) was slowly added and the solution was warmed to 0 °C slowly. After stirring over 1 h, a solution of 4.0 mL of THF solution of *trans*-9-methyl-10-cyano-decalone-3 (**2**) (191 mg, 1.0 mmol) was added dropwise, and the solution was allowed to warm to room temperature for 6 h. The reaction was quenched by saturated NH_4Cl and ether extracted. The combined solvents were washed with water and brine, dried over sodium sulfate and concentrated in vacuo to give the crude material, which was subjected to column chromatography (hexane/ether, 20:1) to give a mixture of **20** and **21** (256 mg, 87%).

A mixture of compound **20** and **21** (100 mg, 0.34 mmol) was added into a mixture of 10% hydrochloric acid (4.0 mL) and THF (4.0 mL) and stirred for 3 h at room temperature. Then the mixture was diluted with saturated $NaHCO_3$ solution and ether extracted. The combined extracts were washed with brine, dried over sodium sulfate, and concentrated in vacuo to give the crude material, which was subjected to column chromatography (hexane/ether, 10:1) to give 82 mg (86%) of **22** as a white solid: mp 176−178 °C; ^{1}H NMR (300 MHz, $CDCl_3$) δ 7.85−7.81 (m, 2H), 7.56−7.50 (m, 1H), 7.47−7.42 (m, 2H), 3.53 (t, J = 6.8 Hz, 1H), 2.39−2.33 (m, 1H), 1.80−1.53 (m, 5H), 1.49−1.38 (m, 2H), 1.35−1.27 (m, 2H), 1.04 (s, 3H); ^{13}C NMR (75 MHz, $CDCl_3$) δ 203.3, 137.2, 132.3, 128.9 (2), 128.7 (2), 122.5, 43.2, 40.4, 36.8, 35.4, 34.9, 32.6, 32.0, 22.5, 20.5, 19.9, 16.5; HRMS-EI m/z (M^+) calcd for $C_{19}H_{23}NO$ 281.1780, found 281.1785.

(*Z*)-3-((*tert*-Butyldimethylsilyloxy)(phenyl)methylidene)-*trans*-8a-methyl-octahydro-naphthalene-4a-carbonitrile (23). To a solution of diisopropylamine (0.15 mL, 1.07 mmol) in 4.0 mL of THF was added 0.43 mL of 2.47 M *n*-BuLi under nitrogen at −78 °C. The reaction mixture was stirred for 30 min and HMPA (0.37 mL, 2.13 mmol) was added and stirred for 15 min. Then a THF solution (2.0 mL) of 3-*endo*-benzoyl-*trans*-8a-methyl-decahydro-naphthalene-4a-carbonitrile (**22**) (100 mg, 0.36 mmol) was slowly added and the reaction mixture was warmed to 0 °C over 1 h. Then 1.5 mL of THF solution of TBSCl (200 mg, 1.3 mmol) was added and stirred for 2 h. The reaction mixture was quenched with water and ether extracted. The combined solvents were washed with water and brine, dried over sodium sulfate, and concentrated in vacuo to give the crude material, which was subjected to column chromatography (hexane/ether, 10:1) to give 130 mg (93%) of **23** as a white solid: mp 104−106 °C; ^{1}H NMR (300 MHz, $CDCl_3$) δ 7.42−7.38 (m, 2H), 7.36−7.28 (m, 3H), 3.03−2.96 (m, 1H), 2.33 (d, J = 14.4 Hz, 1H), 2.11−1.99 (m, 2H), 1.80−1.56 (m, 6H), 1.51−1.26 (m, 4H), 1.06 (s, 3H), 0.89 (s, 9H), −0.08 (s, 3H), −0.26 (s, 3H); ^{13}C NMR (75 MHz, $CDCl_3$) δ 145.8, 138.4, 129.8 (2), 128.2 (2), 127.8, 123.6, 114.3, 46.8, 38.0, 37.3, 35.8, 35.0, 31.2, 26.0, 23.2, 21.9, 20.7, 18.4, 16.5, −4.1, −4.3; HRMS-EI m/z ([M − ^{t}-Bu]$^+$) calcd for $C_{21}H_{28}NOSi$ 338.1940, found 338.1929.

4a-Aminomethylene-*Z*-3-((*tert*-Butyldimethylsilyloxy)(phenyl)-methylidene)-*trans*-8a-methyl-octahydro-naphthalene (24). DIBAL-H (1.5 M in toluene, 0.5 mL, 0.76 mmol) was added to a solution of (*Z*)-3-((*tert*-butyldimethylsilyloxy)(phenyl)methylidene)-*trans*-8a-methyl-octahydro-naphthalene-4a-carbonitrile (**23**) (100 mg, 0.25 mmol) in 2.0 mL of ether at 0 °C. The solution was stirred at this temperature for 1.5 h. $NaBH_4$ (57 mg, 1.5 mmol) was added followed by dropwise addition of 2.0 mL of ethanol. After being stirred at room temperature for 2 h, the reaction mixture was poured into saturated Na_2CO_3 solution and ether extracted. The combined solvents were washed with brine, dried, and concentrated in vacuo. The residue was subjected to column chromatography (from hexane/ether, 1:1 to ethyl acetate) to give 55 mg (55%) of **24**: mp 86−88 °C; ^{1}H NMR (300 MHz, $CDCl_3$) δ 7.33−7.22 (m, 5H), 2.94 (dd, J = 15, 5.4 Hz, 1H), 2.83−2.73 (m, 2H), 2.12 (td, J = 14.1, 6.3 Hz, 1H), 1.91 (d, J = 14.4 Hz, 1H), 1.83 (d, J = 14.4 Hz, 1H), 1.65−1.31 (m, 5H), 1.20−1.13 (m, 2H), 1.16 (s, 3H), 1.11−0.96 (m, 3H), 0.86 (s, 9H), 0.65 (brs, 2H), −0.1 (s, 3H), −0.3 (s, 3H); ^{13}C NMR (75 MHz, $CDCl_3$) δ 143.7, 139.1, 129.5 (2), 128.1 (2), 127.6, 116.9, 40.6, 40.1, 35.6, 34.5, 34.4, 32.6, 27.3, 26.0, 22.1, 21.2, 21.1, 20.6, 18.4, −4.1 (2); HRMS-EI m/z (M^+) calcd for $C_{25}H_{41}NOSi$ 399.2957, found 399.2942.

Kinetic Protonation Study. In a typical run with acetic acid as the proton donor, to the THF solution of *tert*-butyldimethylsilyloxy enol ethers (0.022 M, 0.44 mL) was added acetic acid and followed by 19.4 μL of 1.0 M tetrabutylammonium fluoride in THF. The reaction mixture was stirred at room temperature for 4 h. Then water-dichloromethane quenching and extraction afford a mixture of the *exo*- and *endo*-benzoyl products and the starting material silyl enol ether. The mixture was analyzed by ^{1}H NMR to give the *exo*- and *endo*-benzoyl isomers ratio.

Stability of *endo*-Benzoyl Derivatives under Protonation Conditions. In a typical run, to *endo*-benzoyl derivatives (4.0 mg, 0.013 mmol) dissolved in 0.40 mL of THF was added acetic acid (49 μL, 0.85 mmol), followed by 26.6 μL of tetrabutylammonium fluoride in THF (0.026 mmol, 1.0 M). The reaction mixture was stirred at room temperature. After 4 h, the reaction mixture was diluted with water and dichloromethane extracted. The combined extracts were washed with water and brine, and dried over sodium sulfate, and concentrated in vacuo. The residue was analyzed by ^{1}H NMR. There was no epimerization product observed.

NOE Measurements of (*Z*)-3-Benzylidene-*trans*-8a-methyl-octahydro-naphthalene-4a-carbonitrile (3) and (*E*)-3-Benzylidene-*trans*-8a-methyl-octahydro-naphthalene-4a-carbonitrile (4). With irradiation of the equatorial hydrogen at carbon 1 (δ 2.77 ppm) in the (*Z*)-3-benzylidene-*trans*-8a-methyl-octahydro-naphthalene-4a-carbonitrile (**3**), the proton signal on the aromatic phenyl group (δ 7.35−7.32 ppm) was enhanced. With irradiation of the equatorial hydrogen at carbon 3 (δ 2.25−2.18 ppm) in the (*E*)-3-benzylidene-*trans*-8a-methyl-octahydro-naphthalene-4a-carbonitrile (**4**), the proton signal on the aromatic phenyl group (δ 7.31−7.28 ppm) was enhanced. Thus NOE indicates proximity of these groups in the *Z*-isomer.

Acknowledgment. Support of this research by the National Science Foundation is gratefully acknowledged with special appreciation for its support of basic research as well as to the donors of the Petroleum Research Fund, administered by the American Chemical Society.

Supporting Information Available: General procedures, kinetic data, vector analysis of hybridization, computational data, X-ray data including CIF file, and ^{1}H and ^{13}C NMR spectra. This material is available free of charge via the Internet at http://pubs.acs.org.

JO051611I